

Graveyard Effects of Antimicrobial Nanostructured Titanium Over Prolonged Exposure to Drug Resistant Bacteria and Fungi

Louisa Z. Y. Huang,¹ Rowan Penman,¹ Rashad Kariuki,¹ Pierre H. A Vaillant,¹ Soroosh Gharehgozlo,¹ Z. L Shaw,² Vi Khanh Truong,³ Jitraporn Vongsvivut,⁴ Aaron Elbourne,^{1*} and Rachel A. Caruso^{1*}

¹ School of Science, College of STEM, RMIT University, Melbourne, Victoria 3000, Australia

² School of Engineering, College of STEM, RMIT University, Melbourne, Victoria 3000, Australia

³ Healthcare Engineering Innovation Group, Department of Biomedical Engineering & Biotechnology, College of Medicine and Health Science, Khalifa University, Abu Dhabi, UAE

⁴ Infrared Microspectroscopy Beamline, ANSTO – Australian Synchrotron, Clayton, Victoria 3168, Australia.

Supplementary Information

Table S1. Surface measurements of control and nanostructured titanium surfaces.

Sample	RMS Sa (nm) ^a	Width (nm) ^{a,b}	Length (nm) ^a	Interspacing (nm) ^{a,b}	Height (nm) ^a	Aspect Ratio ^c
Control	102.2	-	-	-	-	-
Nanostructured	104.6	40.3 ± 15.8	186.4 ± 49.3	193.7 ± 125.0	210.1 ± 73.4	5.2 ± 1.3

^{a)} Derived from AFM; ^{b)} Derived from SEM; ^{c)} Derived from length and width measurements.
RMS = root mean squared, Sa = arithmetical mean height.

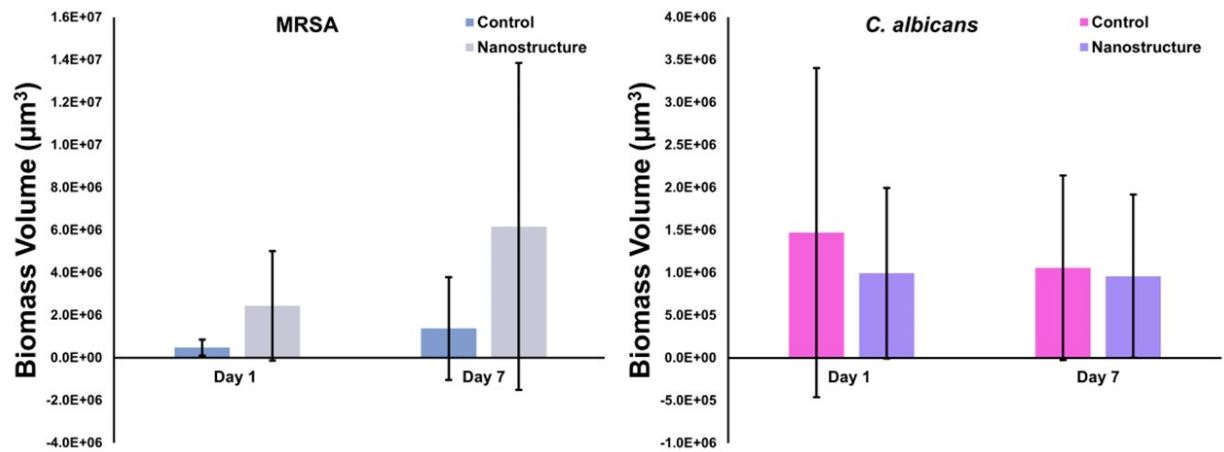


Figure S1. Biomass growth determined from CLSM analysis of MRSA (left) and *C. albicans* (right) on control and nanostructured titanium showing that a large variation in the data is caused by experimental replicates using different parent inoculates. As this study is sensitive to biofilm growth, it is important to control the differing factors that may influence greater or lesser growth to purely understand the influence of the surface on the growth.

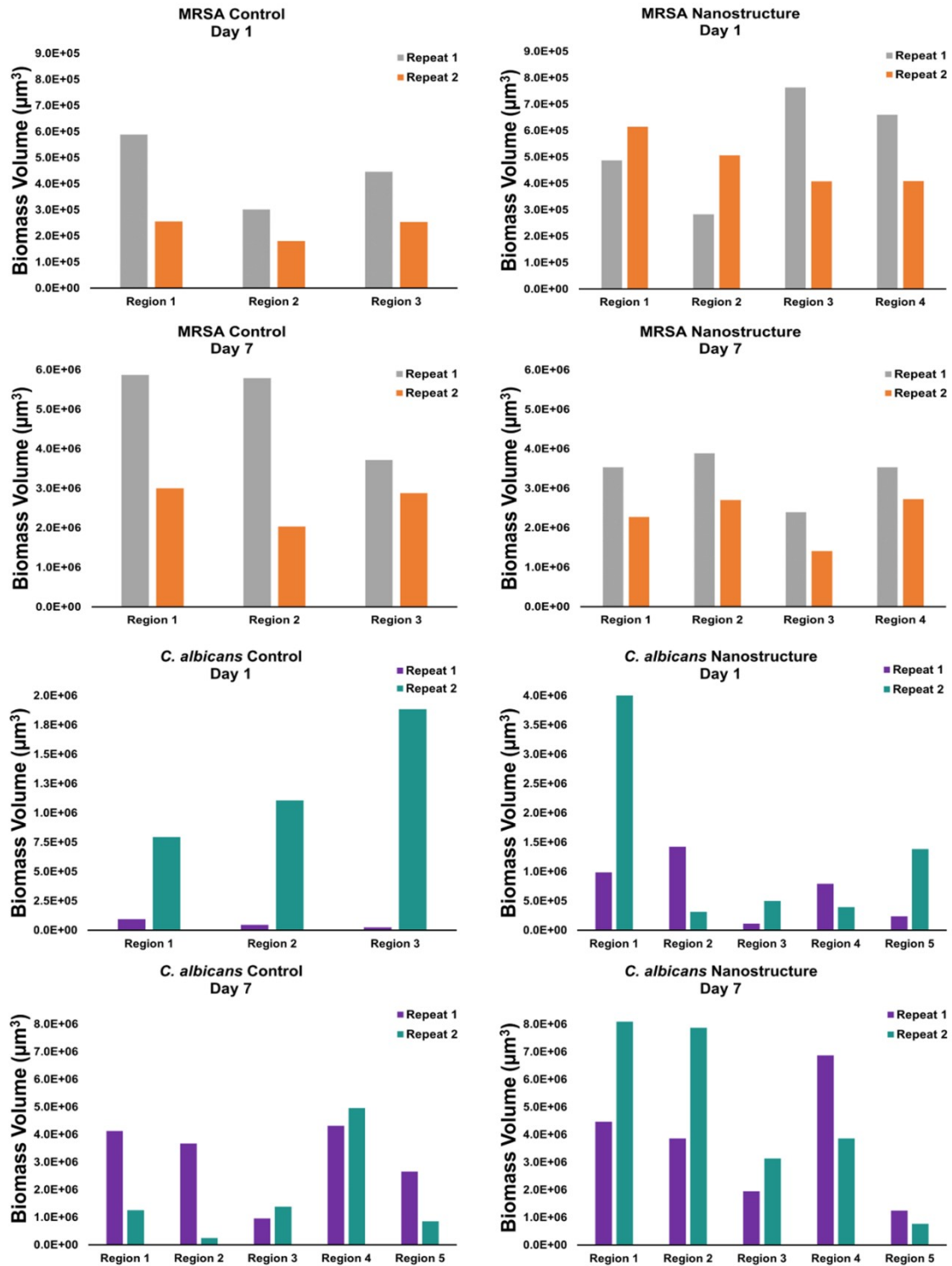


Figure S2. Biomass growth was determined using CLSM of MRSA and *C. albicans* on control and nanostructured titanium for each region on a sample replication as described in Figure 2. Samples with more than three regions displayed large visual variation in growth over the titanium surface, therefore the number of areas was increased for a better overview of the sample. Note: 'Region 1,2,3...' does not indicate identical coordinates on each sample but is a placeholder for the different areas imaged on a single surface.

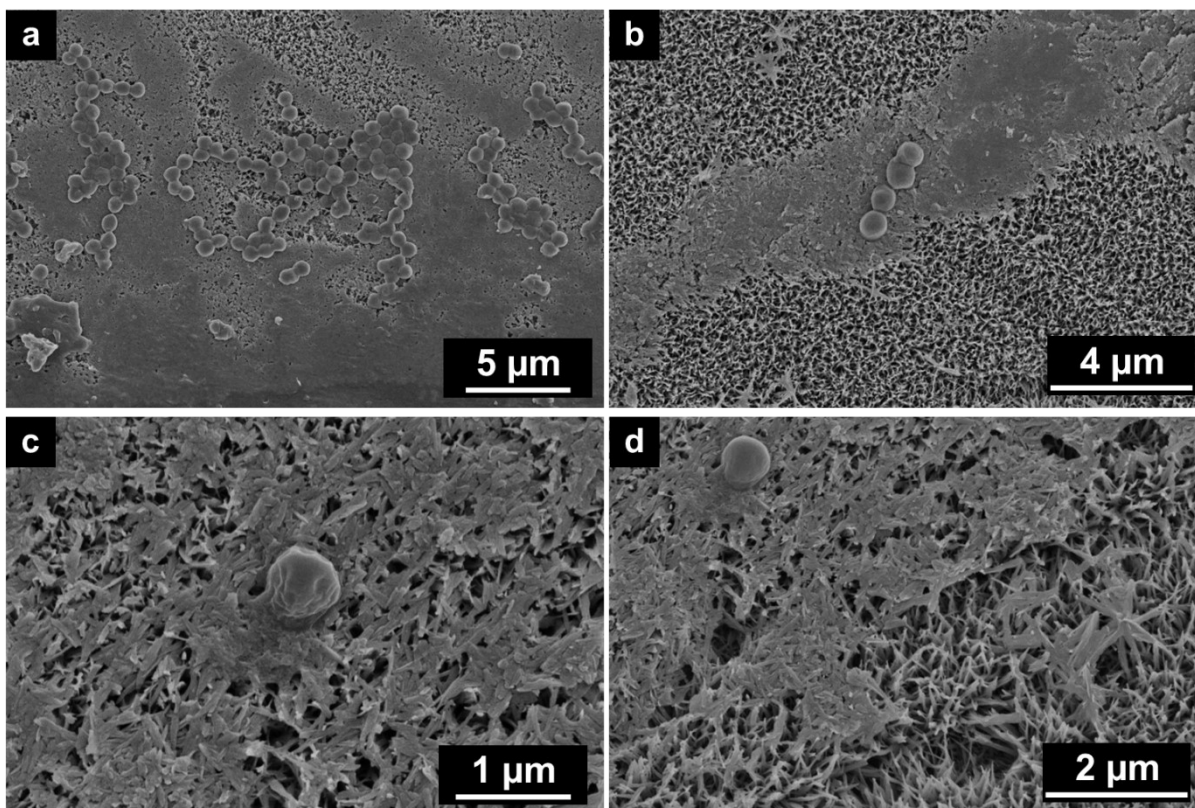


Figure S3. a) Low resolution SEM image of MRSA on nanostructured titanium after 1 day of exposure. b) EPS-covered nanostructures with MRSA cells adhered atop. c-d) MRSA observed forming EPS.

Table S2. Average integral absorbance of the outlined regions for MRSA. All values are extremely statistically significant (p -value < 0.0001) when comparing the control and nanostructured surfaces at each time point, control at day 1 and control at day 7, and nanostructured at day 1 and nanostructured at day 7. $N = 3500, 3000, 2500,$ and 3500 for control titanium at day 1, nanostructured titanium at day 1, control titanium at day 7 and nanostructured titanium at day 7.

MRSA	Day 1		Day 7	
	Control	Nanostructured	Control	Nanostructured
Lipids (CH₂/CH₃) 2980—2800 cm⁻¹	0.8 ± 0.5	1.5 ± 0.9	0.8 ± 0.6	0.4 ± 0.5
Proteins (Amide I) 1695—1590 cm⁻¹	3.9 ± 1.5	5.1 ± 2.4	3.5 ± 1.9	4.7 ± 3.0
Polysaccharides 1175—1000 cm⁻¹	0.5 ± 0.9	2.5 ± 1.3	2.9 ± 2.2	1.0 ± 1.5

Table S3. Average integral absorbance of the outlined regions for *C. albicans*. Most values are extremely statistically significant (p-value < 0.0001) when comparing the control and nanostructured surfaces at each time point, control at day 1 and control at day 7, and nanostructured at day 1 and nanostructured at day 7 at a significance level of 0.05. * denotes p value was not statistically significant when comparing nanostructured titanium with the control titanium at the same time point. *N* = 3500, 3000, 2500, and 3500 for control titanium at day 1, nanostructured titanium at day 1, control titanium at day 7 and nanostructured titanium at day 7.

<i>C. albicans</i>	Day 1		Day 7	
	Control	Nanostructured	Control	Nanostructured
Lipids (CH₂/CH₃) 2980—2800 cm⁻¹	1.7 ± 0.9	1.7 ± 0.5*	0.8 ± 0.4	1.7 ± 0.6
Proteins (Amide I) 1695—1590 cm⁻¹	2.3 ± 1.4	2.6 ± 0.7	1.3 ± 0.5	2.5 ± 0.7
Polysaccharides 1175—1000 cm⁻¹	2.1 ± 1.1	2.6 ± 0.9	2.1 ± 0.7	3.1 ± 0.9

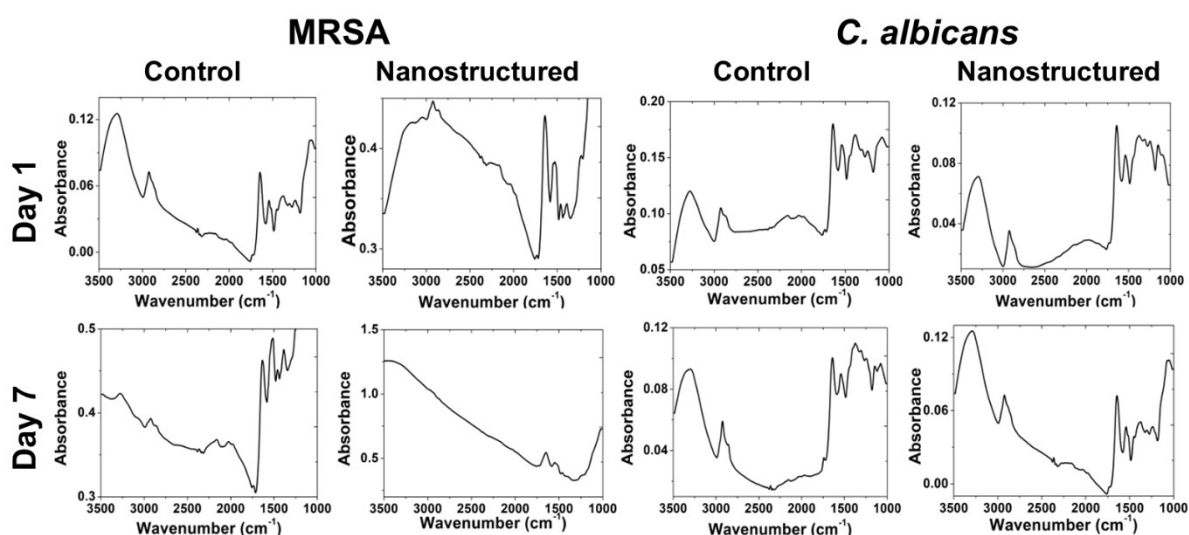


Figure S4. HCA average spectra obtained from synchrotron macro ATR-FTIR spectroscopy used for PCA analysis for MRSA (left) and *C. albicans* (right) atop control titanium (top row) or nanostructured titanium (bottom row) at 1 day and 7 days.

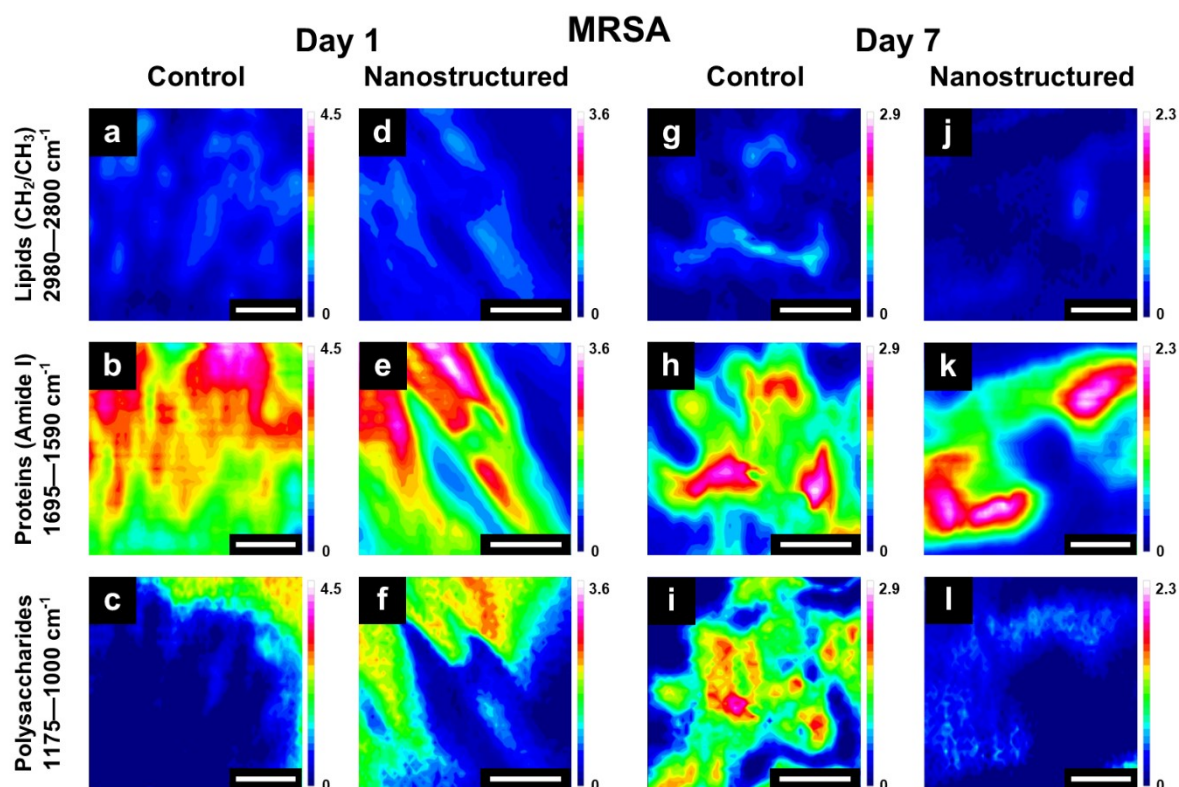


Figure S5. Synchrotron macro ATR-FTIR chemical maps observed for MRSA at day 1 (a-f) and day 7 (g-l) on control titanium and nanostructured titanium, which were obtained by integrating areas under $\nu(\text{C-H})$ peaks of CH_2/CH_3 groups for lipids (top row), amide I band for proteins (middle row), and $\nu(\text{C-O})/\nu(\text{C-C})$ peaks of polysaccharides (bottom row). Colour scale from dark blue to white corresponds to minimum to maximum integrated peak values. Scale bar represents 20 μm .

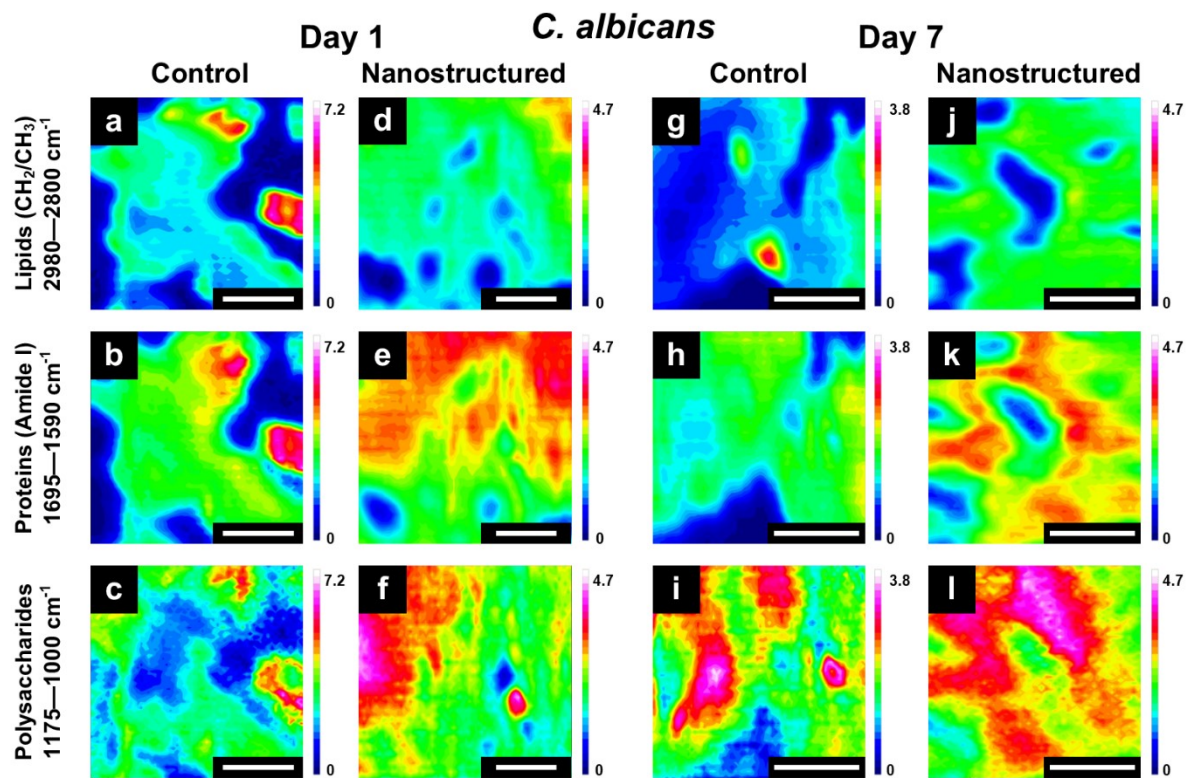


Figure S6. Synchrotron macro ATR-FTIR chemical maps observed for *C. albicans* at day 1 (a-f) and day 7 (g-l) on control titanium and nanostructured titanium, which were obtained by integrating areas under $\nu(\text{C-H})$ peaks of CH₂/CH₃ groups for lipids (top row), amide I band for proteins (middle row), and $\nu(\text{C-O})/\nu(\text{C-C})$ peaks of polysaccharides (bottom row). Colour scale from dark blue to white corresponds to minimum to maximum integrated peak values. Scale bar represents 20 μm .